J Mater Sci (2009) 44:3719–3730
DOI 10.1007/s10853-009-3497-5

Polymerization in sodium silicate solutions: a fundamental process in geopolymerization technology

D. Dimas · I. Giannopoulou · D. Panias

Received: 15 January 2009 / Accepted: 11 April 2009 / Published online: 6 May 2009

Abstract Geopolymerization is an innovative technology that can transform several solid aluminosilicate materials into useful products called geopolymers or inorganic polymers. Although the geopolymerization mechanism is not well understood, the most proposed mechanism includes four parallel stages: (a) dissolution of solid aluminosilicate materials in alkaline sodium silicate solution, (b) oligomerization of Si and/or Si–Al in aqueous phase, (c) polymerization of the oligomeric species, and (d) bonding of undissolved solid particles in the polymer. It is obvious that polymerization in sodium silicate solutions comprises a fundamental process in geopolymerization technology. Therefore, this article aims at studying experimentally the polymerization stage in synthetic pure sodium silicate solutions. The structure of sodium silicate gels as a function of the SiO_2/Na_2O molar ratio is examined and their hardness as well as hydrolytic stability are determined. In addition, the effect of aluminum incorporation in the hydrolytic stability of these gels is also examined. Finally, the structure of sodium silicate and aluminosilicate gels is correlated to the measured properties drawing very useful conclusions that could be applied on geopolymerization technology.

Introduction

A new technology able to absorb substantial quantities of water-soluble silicates has emerged during the last two decades. This is the so-called geopolymerization technology. Geopolymerization is an innovative technology that can transform several aluminosilicate materials into useful products called geopolymers or inorganic polymers. Geopolymerization involves a heterogeneous chemical reaction between solid aluminosilicate oxides and alkali metal silicate solutions at highly alkaline conditions and mild temperatures yielding amorphous to semi-crystalline polymeric structures, which consist of Si–O–Al and Si–O–Si bonds [1]. A variety of industrial minerals [2, 3], such as kaolinite, feldspars, and etc., and industrial solid residues or wastes [4–9], such as fly ashes, metallurgical slags, mine wastes, etc., have been used as solid raw materials in the geopolymerization technology. The vast majority of water-soluble alkali silicates used in geopolymerization is sodium silicates because they are cheaper and produced in substantially larger quantities than the potassium silicates. Geopolymers possess excellent physico-chemical and mechanical properties, including high strength, micro- or nano-porosity, negligible shrinkage, thermal stability, high surface hardness, fire, and chemical resistance [10].

The geopolymerization mechanism is not well understood. The most proposed mechanism includes the following stages, which proceed in parallel and thus, are impossible to be distinguished.

(i) Dissolution of the solid aluminosilicate materials in the strong alkaline aqueous solution.

During this stage Si and Al are transferred from the solid phase to the aqueous one. For some researchers [11, 12], the dissolution results in the generation of soluble aqueous monomeric species of Si and Al. This type of dissolution is called congruent. For some other researchers [10, 13], the dissolution results in the release of oligomeric molecular units having composition, which is dependent on the type of the

D. Dimas · I. Giannopoulou · D. Panias (✉)
Laboratory of Metallurgy, School of Mining and Metallurgical Engineering, National Technical University of Athens, 15780 Zografou, Athens, Greece
e-mail: panias@metal.ntua.gr

solid aluminosilicate raw material. This type of dissolution is called incongruent. There are not enough data to exclude either of the dissolution types. In the case of dissolution of industrial aluminosilicate minerals such as kaolinite and feldspars, the incongruent type seems to be predominant. In the case of waste aluminosilicate materials with complex composition, the congruent type seems to predominate.

(ii) Formation of Si and/or Si–Al oligomers in the aqueous phase.

In case of congruent type of dissolution, certain chemical reactions take place between the soluble aqueous monomeric species of Si and Al, resulting in the formation of the geopolymers precursors which are oligomeric species (polynuclear hydroxy-complexes) consisting of polymeric bonds of Si–O–Si and Si–O–Al type [7, 14]. This stage has been bypassed in case of incongruent type of dissolution, supporting a faster geopolymerization process provided that the product of dissolution is the oligomeric molecular units.

(iii) Polycondensation of the oligomeric species or units in the aqueous phase to form an inorganic polymeric material.

Independently of the dissolution type, polycondensation is the basic chemical process forming mainly a gelatinous phase which represents the core of the polymeric materials.

(iv) Bonding of undissolved solid particles in the final geopolymeric structure.

This article aims at studying experimentally the polycondensation stage in synthetic pure sodium silicate solutions. Especially, it aims to study the structure of gelatinous phase as a function of the SiO_2/Na_2O molar ratio through its examination with X-ray diffraction, thermogravimetric & differential thermal analysis, Fourier-transform infrared spectroscopy (FTIR), and scanning electron microscopy (SEM). In addition, the hardness and the hydrolytic stability of formed gelatinous phase will be determined as a function of the SiO_2/Na_2O molar ratio and the effect of aluminum addition on the hydrolytic stability of the formed gelatinous phase will be examined through some preliminary experiments. Finally, the structure of gelatinous phase will be correlated to the measured properties, drawing very useful conclusions that could be applied on geopolymerization technology.

Materials and methods

The experimental polymerization procedure was performed in two discrete steps. The first step included the preparation of the sodium silicate solution with a pre-fixed SiO_2/Na_2O molar ratio (R_M). The standard sodium silicate solution was a commercial water-glass solution with $R_M = 3.48$ and density 1346 kg/m^3 supplied by Merck. Sodium silicate solutions with higher SiO_2/Na_2O molar ratios were prepared by dissolving silicon (IV) oxide amorphous fumes (purity 99.8% and surface area 300–350 m^2/g) supplied by Alfa Aesar in the standard water-glass solution. Sodium silicate solutions with lower SiO_2/Na_2O molar ratios were prepared by dissolving pure NaOH pellets supplied by Merck in the standard water-glass solution. In some experiments aluminum was added in the sodium silicate solution in the form of aluminum chloride or sodium aluminate solutions in order to prepare an initial aqueous phase with a pre-fixed Si/Al molar ratio.

The second step included the formation of silicate gels by accelerated polycondensation in sodium silicate or aluminosilicate solutions. Accelerated polycondensation was performed in an electrical oven equipped with a diaphragm vacuum pump at 60 °C by gradual evaporation of water. The vacuum oven was operated on daily cycles. Each cycle consisted of 2 h evaporation under vacuum followed by 1 h evaporation at atmospheric pressure repeated thrice and then 15 h evaporation at atmospheric pressure. The whole duration of each polycondensation experiment comprised five daily cycles during which 80–85% of the initially contained water was evaporated.

The structure of gelatinous silicate phase was determined by means of X-ray diffractometry (XRD) utilizing a Siemens D5000 diffractometer, FTIR utilizing a Perking Elmer 880 spectrometer, thermal analysis (TG/DTA) utilizing a Setaram Labsys analyzer, and SEM utilizing a Jeol JSM-type SEM.

The Vickers hardness of silicate gels was measured in a Vickers hardness tester of Zwick/Roell by applying a load of 10 kg on a flat surface that was prepared by grinding and polishing the solid gelatinous material which was incorporated in a synthetic resin.

The hydrolytic stability of gelatinous silicate phase was determined through a dissolution test in deionized water. An aliquot of 2 g of silicate gel was totally immersed in 100 mL of deionized water and let in contact for 24 h at ambient temperature. After pH measurements, the solution was filtrated and analyzed for its silicon and in some cases aluminum content by inductively coupled plasma mass spectrometer.

Results and discussion

Gelatinous phase structure

The XRD patterns of the sodium silicate gels formed at different SiO_2/Na_2O molar ratios are shown in Fig. 1. The

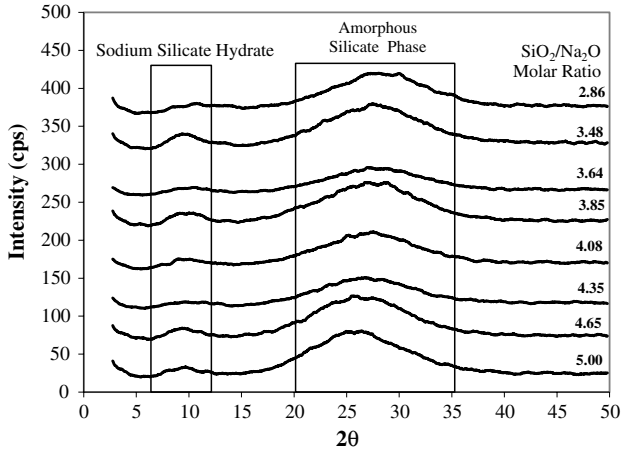

Fig. 1 XRD patterns of sodium silicate gels as a function of SiO_2/Na_2O molar ratio

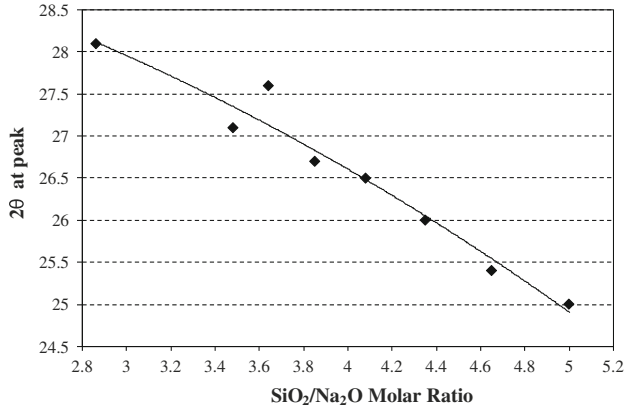

Fig. 2 Dependence of angle 2θ of halo peak on SiO_2/Na_2O molar ratio of sodium silicate gels

silicate phases were characterized as X-ray amorphous materials. There was a lack of sharp diffraction peaks in the X-ray diffractograms which were consisted of only two broad diffuse halo peaks or broad humps. The most intense halo peak was registered between $2\theta = 20°$ and $2\theta = 35°$ and was attributed to an amorphous silicate phase consisting of a SiO_4 tetrahedra sharing oxygen atoms and lacking any long-range order [15–18]. The position of this halo peak in amorphous sodium silicate phases is strongly related to the structural organization of the SiO_4 tetrahedra on the scale of their first coordination shell [15]. The XRD pattern of a highly polymerized pure silica (molar ratio $SiO_2/Na_2O = \infty$) with 3D-framework structure consisting exclusively of SiQ^4 structural units (all oxygen atoms in the first coordination sphere of Si atom are bridging oxygen atoms) has a halo peak at $2\theta = 21.3°$ [15, 18]. As the number of network modifying sodium atoms per silicon atom increases (the molar ratio SiO_2/Na_2O decreases), the number of non-bridging oxygen (NBO) atoms in the first coordination sphere of Si atoms also increases, resulting in substantial structural changes in the amorphous sodium silicate phase. The XRD pattern of a Na_2O–SiO_2 model glass (molar ratio $SiO_2/Na_2O = 1$) with a (–O–Si–O–Si–O–)$_n$ chain structure consisting exclusively of SiQ^2 structural units (only two oxygen atoms in the first coordination sphere of Si atom are bridging oxygen atoms) has a halo peak at $2\theta = 34°$ [15, 18]. This systematic shift of the halo peak toward lower 2θ angles with increasing SiO_2/Na_2O molar ratios (Fig. 2) was observed also in the gelatinous sodium silicate phases prepared in this study. The sodium silicate phase prepared at the lowest studied molar ratio $SiO_2/Na_2O = 2.86$ had a halo peak at $2\theta = 28.1°$, whereas the one prepared at the highest molar ratio $SiO_2/Na_2O = 5$ had a halo peak at $2\theta = 25°$. The halo peaks of the sodium silicate gels at intermediate molar ratios were located in-between the two extreme 2θ values. The explanation of the experimental results was based on the understanding of silicon chemistry in aqueous solutions.

In acidic, neutral, and mild alkaline aqueous solutions silicon occurs predominantly as $Si(OH)_4^0$ neutral species [19, 20]. In high alkaline aqueous solutions (pH > 9), the following general deprotonation reaction (Eq. 1) governs at significant extent the aqueous equilibria [19, 20]:

$$Si(OH)_4^0 + jOH^- = \left[SiO_j(OH)_{4-j}\right]^{j-} + jH_2O \qquad (1)$$

At high silicon concentration in the aqueous solutions, which occurs only at high pH values (pH > 10) [20], oligomerization of monomers (Eq. 2) followed by deprotonation (Eq. 3) and polycondensation (Eq. 4) reactions governs the aqueous equilibria [19–22]:

$$kSi(OH)_4^0 = \left[Si_kO_l(OH)_{4k-2l}\right]^0 + lH_2O \quad 2 \le k \le 8, \qquad (2)$$

where, l denotes the number of bridging oxygens (–Si–O–Si–)

$$\left[Si_kO_l(OH)_{4k-2l}\right]^0 + mOH^- + mNa^+ = \left[Si_kO_{l+m}(OH)_{4k-2l-m}\right]^{m-} \cdot mNa^+ + mH_2O, \qquad (3)$$

where, m denotes the number of singly-negatively charged oxygen anions

$$n\left(\left[Si_kO_{l+m}(OH)_{4k-2l-m}\right]^{m-} \cdot mNa^+\right) = \left[Si_{nk}O_{n(l+m)+w}(OH)_{n(4k-2l-m)-2w}\right]^{nm-} \cdot nmNa^+ + wH_2O, \qquad (4)$$

where, n denotes the polymerization degree.

The structure of produced gelatinous silicate phases is modified by the presence of sodium ions. Due to the strong deprotonation reactions taking place in high alkaline solutions, the oligomers contain singly-negatively charged oxygen anions that attract sodium cations, creating thus alkaline NBO sites (Eq. 3). Therefore, the incorporation of

alkali metal ions on interstitial sites is unavoidable during silicon polycondensation in the presence of alkali metal ions [23, 24]. The amount of NBO sites is a function of the SiO_2/Na_2O molar ratio in the prepared silicate gels. Low SiO_2/Na_2O molar ratio is equivalent with increased number of NBO sites and thus with structures consisting principally of SiQ^2, SiQ^1 structural units which form silicate chains, dimers, and monomers. On the contrary, high SiO_2/Na_2O molar ratio is equivalent with decreased number of NBO sites and thus with structures consisting principally of SiQ^3, SiQ^4 structural units which form silicate 3D frameworks and sheets. In the case of the gelatinous silicate phase with the highest molar ratio $SiO_2/Na_2O = 5$, the position of the halo peak indicates the predominance of SiQ^3 units which create a mixed structure consisting of silicate sheets and 3D frameworks [15]. The position of the halo peak in the gelatinous silicate phase with the lowest molar ratio $SiO_2/Na_2O = 2.86$ indicates the predominance of SiQ^2 units that create a mixed silicate chains and sheets structure [15].

This latter conclusion was also strengthened by the FTIR analysis of produced sodium silicate gels. The IR spectrum is divided in two ranges: (a) 370–1300 cm^{-1} which is related to the vibrational modes of –Si–O–Si– units and (b) 1600–4000 cm^{-1} which is related to the vibrational modes of adsorbed water. The IR spectra of gelatinous silicate phases at different SiO_2/Na_2O molar ratios in the range 370–1300 cm^{-1} are shown in Fig. 3. There are three main bands attributed to different vibrations in the –Si–O–Si– units [7, 25]: (a) 1000–1100 cm^{-1} due to asymmetric stretching (band I), (b) 750–800 cm^{-1} due to symmetric stretching (band II), and (c) $\approx$460 cm^{-1} due to bending (band III). The three above bands were observed in the IR spectra of the gelatinous sodium silicate phases shown in Fig. 3. All observed bands were very broad absorption bands, indicating the structural disorder in the silicate network and thus the amorphous character of the gelatinous silicate phases. Especially, the band I, which is mentioned as the footprint of geopolymerization [1, 7, 10], was very broad extending in the range 850–1200 cm^{-1}. The broadness of this band reflected the wide distribution of SiQ^n structural units in the sodium silicate gels. It is well known that the stretching vibrations of the –Si–O–Si– bonds of the SiQ^n structural units are IR active in the range 850–1200 cm^{-1} [26, 27]. Especially, the SiQ^4 unit shows IR absorption band centered around 1200 cm^{-1}, the SiQ^3 unit around 1100 cm^{-1}, the SiQ^2 unit around 950 cm^{-1}, the SiQ^1 unit around 900 cm^{-1}, and the SiQ^0 unit around 850 cm^{-1}. The broad IR spectra in the range 850–1200 cm^{-1} of Fig. 3 were the result of the overlapping of the five individual absorption bands of the SiQ^n structural units. Resolution of the specific SiQ^n absorption bands in the obtained IR spectra was not detected. The IR spectra showed a maximum absorption band in the range 1000–1050 cm^{-1} which is consistent with the predominance of SiQ^2 and SiQ^3 structural units over SiQ^0, SiQ^1, and SiQ^4 ones. It is well known that in the structure of highly polymerized sodium silicate gels the SiQ^2 units can form chains and/or rings. The silicooxygen ring vibrational bands occur in the wavenumbers region 500–800 cm^{-1} [25, 27, 28]. Especially, the three-membered rings have a band located at 700–720 cm^{-1}, the four-membered rings exhibit an absorption band at around 650 cm^{-1} and the six-membered rings have a band occurring at 600–620 cm^{-1}. In the IR spectra of Fig. 3, the silicooxygen ring vibrational bands were not resolved. Two very weak, broad, and almost

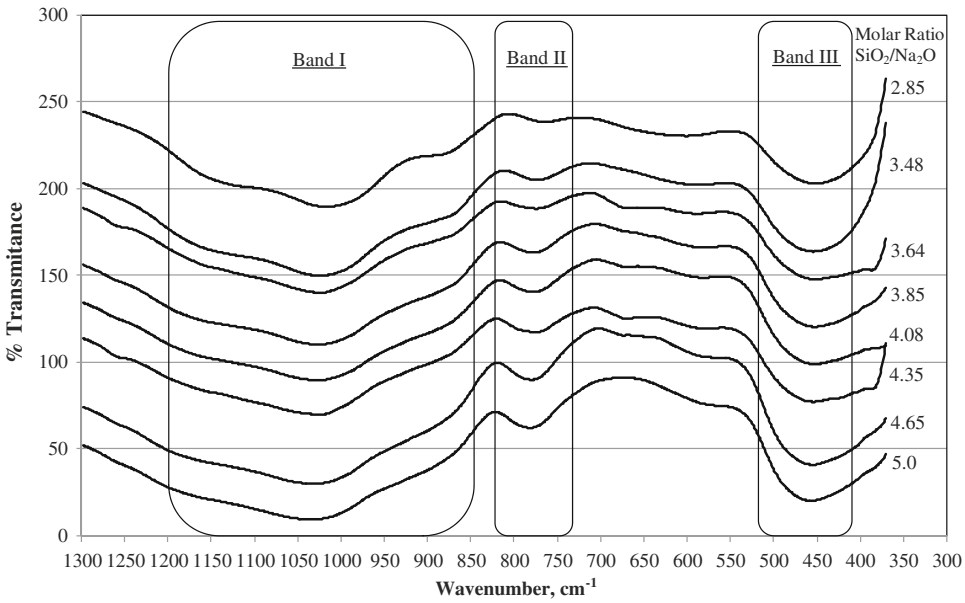

Fig. 3 FTIR spectra of produced sodium silicate gels at different SiO_2/Na_2O molar ratios in the range 370–1300 cm^{-1}

indistinct absorption bands could be observed around 650 and 600 cm^{-1}, indicating that the cyclic structures in the synthesized gelatinous sodium silicate phases were almost absent. The systematic shift of the maximum absorption band toward higher wavenumbers, as the SiO_2/Na_2O molar ratio increased (Fig. 4), indicated the predominance of SiQ^3 structural unit over the SiQ^2 one in the produced gelatinous silicate phases. This systematic shift was valid not only in the band I, but also in the bands II and III as is shown in Fig. 4.

The second broad diffuse halo peak that is observed in Fig. 1 was located in-between $2\theta = 7$ to 12° and was attributed to an amorphous or nanocrystalline sodium silicate hydrate phase. This phase was a minor phase not exceeding 4 wt% of produced sodium silicate gel. It was generated by precipitation during the tests of accelerated polycondensation in sodium silicate solutions. The two phases that were formed during polycondensation can be clearly seen in Fig. 5a. The major phase was an amorphous polymeric phase comprising the matrix of the whole

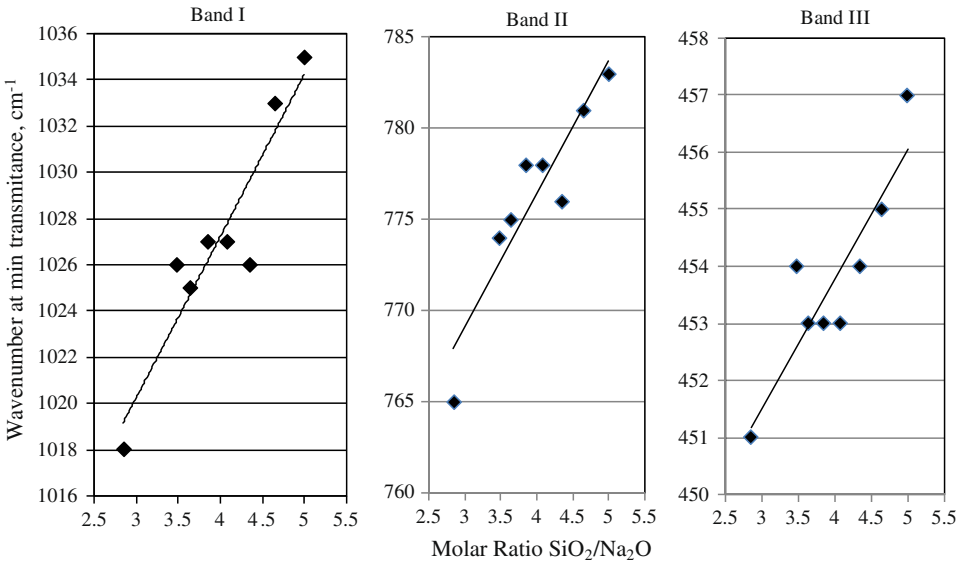

Fig. 4 Shift of the maximum absorption band as a function the SiO_2/Na_2O molar ratio in the sodium silicate gels

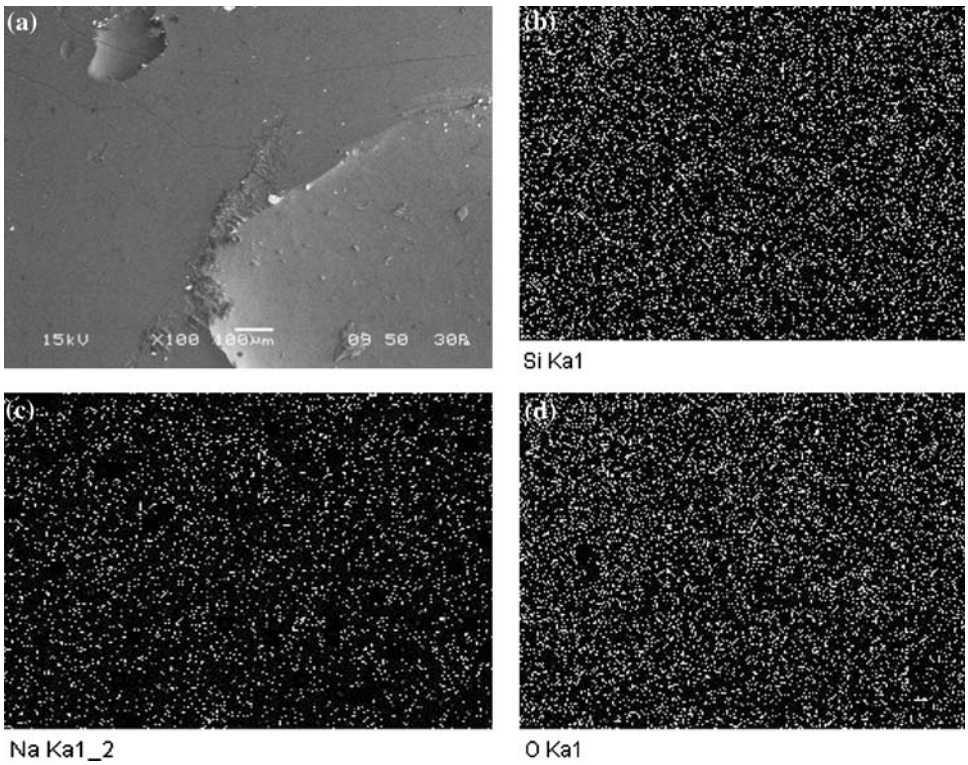

Fig. 5 **a** SEM micrograph of the sodium silicate gel with molar ratio $SiO_2/Na_2O = 5$ and EDS mapping of **b** Si, **c** Na, and **d** O in the micrograph area showing the elements distribution

material. The secondary sodium silicate hydrate phase was observed in the form of agglomerated precipitates with size ranging from 500 nm to 40 μm. Energy dispersive spectroscopy (EDS) mapping of the micrograph area (Fig. 5b–d) showed similar distribution mode for silicon, sodium, and oxygen, indicating that the sodium silicate gel was a homogeneous material.

The XRD diagrams of gelatinous sodium silicate phases (Fig. 1) did not reveal the presence of crystalline sodium hydroxide. Therefore, it was concluded that sodium cations were consumed primarily as network modifying agents in the formation of polymeric material and secondarily for the formation of the sodium silicate hydrate precipitate.

During the polycondensation experiments 80–85% of initially contained water was evaporated. The remaining water in the sodium silicate gels was consumed for the formation of the surface silanol groups or was physically bound by hydrogen bonds to all types of surface silanol groups as it was confirmed by infrared and thermogravimetric analysis. The IR spectra of sodium silicate gels for different SiO_2/Na_2O molar ratios are shown in Fig. 6 in the range of wavenumbers 1500–4000 cm^{-1} where the major vibrational absorption bands of water and SiOH groups are located. The surface silanol groups have characteristic OH stretching vibrations in the spectra region from 3100 to 3800 cm^{-1}. The IR spectra showed a very weak absorption band at around 3750 cm^{-1} assigned to isolated non-interacting surface silanol groups [23, 29–31]. This very weak band showed that the single surface silanols were negligible in almost all the sodium silicate gels. The second feature of the IR spectra shown in Fig. 6 was the broadband located in the range of wavenumbers 3400–3700 cm^{-1} where the absorption bands of internal adjacent hydrogen bonded silanol groups (3640–3660 cm^{-1}) and of surface vicinal hydrogen bonded silanol groups (3530–3550 cm^{-1}) are detected [23, 29–31]. The maximum absorption of this broadband was centered in the region 3400–3460 cm^{-1} which was located outside the region where the above-mentioned silanol groups exhibit their absorption bands. This observation proved the presence of another IR active group in this region that predominated over the internal and vicinal hydrogen bonded silanol groups in the sodium silicate gels. It is well known that the surface physically bound water on silanol groups has absorption bands in the region 3400–3460 cm^{-1} as well as around 1630 cm^{-1} [29, 31]. Although the former band could not be resolved due to interferences in the broadband in-between 3400 to 3700 cm^{-1}, the latter was resolved in the IR spectra of all gelatinous sodium silicate phases shown in Fig. 6, proving the presence of the surface physically bound water on silanol groups. The above conclusions were confirmed also by the results of the thermal analysis (TG/DTA). Typical TG/DTA curves are shown in Fig. 7 for the gelatinous sodium silicate phase with molar ratio $SiO_2/Na_2O = 5$. It was clearly observed that water removal took place in two different stages. The water removal in the first stage took place around 100–115 °C, was completed at about 150 °C, and was accompanied by a strong endothermic peak. This was attributed to physically bound water on silanol groups [23, 29] which can be easily removed from the sodium silicate gel surface at low temperatures. At temperatures higher than 150 °C the dehydroxylation by condensation of surface hydroxyl groups from the internal and vicinal hydrogen bonded silanol groups began [23, 29, 30], which was completed at 500 °C as seen in Fig. 7. According to

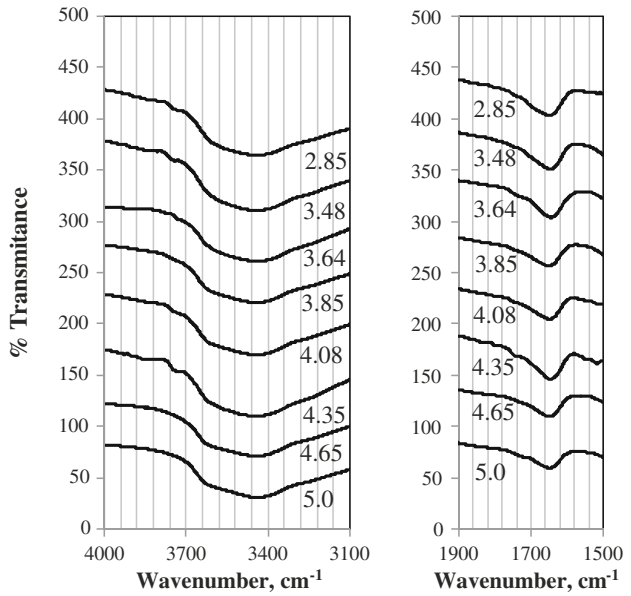

Fig. 6 FTIR spectra of sodium silicate gels at different SiO_2/Na_2O molar ratios in the range 1500–4000 cm^{-1}

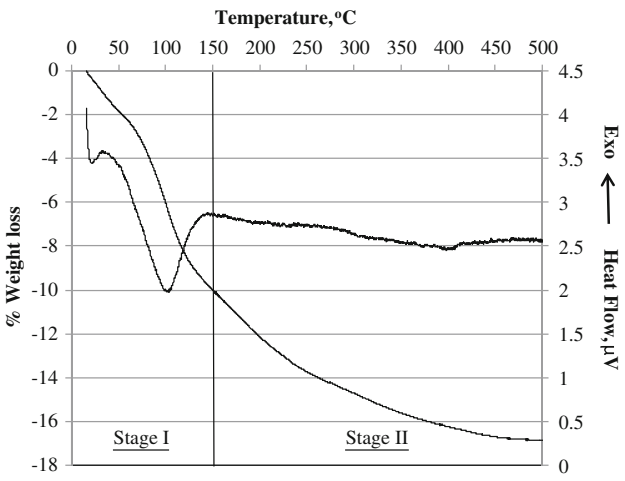

Fig. 7 Thermogravimetric analysis of sodium silicate gel with molar ratio $SiO_2/Na_2O = 5$ (argon atmosphere, rate of temperature increase: 1 °C/min)

literature [23], the water that remained in sodium silicate gel at temperatures higher than 500 °C was attributed to single (isolated) silanol as well as to silanediol (geminal) groups which necessitate substantial higher temperatures to be dehydroxylated. Taking into account the results of the thermogravimetric tests and the water content of the produced sodium silicate gels, it was calculated that 57% of water contained in sodium silicate gels was associated with physically bound water on silanol groups, 39% was related to surface hydroxyl groups from the internal and vicinal hydrogen bonded silanol groups and the remaining 4% was associated with the isolated non-interacting surface silanol groups.

Gelatinous phase properties

The hydrolytic stability of the gelatinous sodium silicate phases was evaluated through dissolution tests. The results are shown in Fig. 8 where the percent silicon dissolution is plotted as a function of the SiO_2/Na_2O molar ratio in the gelatinous sodium silicate phases. The results showed that the sodium silicate gels did not have the same hydrolytic stability. Three different regions were defined. The sodium silicate gels with SiO_2/Na_2O molar ratio <3.5 were totally soluble in water. The ones with SiO_2/Na_2O molar ratio in-between 3.5 to 4.4 had substantial solubility in water which diminished from 100% at molar ratio 3.5 to 15% at molar ratio 4.4. Finally, the sodium silicate gels with molar ratio higher than 4.4 had solubility <10% and therefore were characterized as practically insoluble in water. This behavior was correlated to the gelatinous sodium silicate phase structure. As the SiO_2/Na_2O molar ratio decreased, a shift in the prevailing structural units was observed from SiQ^3 at molar ratio 5 to SiQ^2 at molar ratio 2.86. This structural shift was accompanied by an increased number of sodium NBO interstitial sites ($\equiv$SiONa). The addition of water to sodium silicate gels caused hydrolysis and leached out a part of incorporated sodium according to the following reaction (Eq. 5).

$$\equiv SiONa^0 + H_2O \;=\; \equiv SiOH^0 + Na^+ + OH^- \qquad (5)$$

This reaction produced alkalinity which was measured in the final solutions of the dissolution tests and can be seen in Fig. 9, where the final solution pH is plotted against SiO_2/Na_2O molar ratio. The final solution pH was almost constant at value 10.6 in case of gels with molar ratio higher than 4.4. As the molar ratio decreased, the solution pH increased substantially reaching a value higher than 11.6 in the sodium silicate gel with molar ratio 2.86. The strong alkaline environment attacked the amorphous sodium silicate structures with molar ratio <4.4 causing substantial or total dissolution [32] according to the following reactions (Eqs. 6–8)

$$\equiv Si{-}O{-}Si\equiv + OH^- \;=\; \equiv SiOH^0 + \equiv Si{-}O^-, \qquad (6)$$

$$\equiv SiOH^0 + OH^- \;=\; \equiv Si{-}O^- + H_2O, \qquad (7)$$

$$\equiv Si{-}O^- + H_2O = SiOH^0 + OH^-. \qquad (8)$$

The Vickers hardness of the gelatinous sodium silicate phases is shown in Fig. 10 as a function of the SiO_2/Na_2O molar ratio. It was clearly observed that the hardness followed an exponential function of molar ratio. The practically insoluble sodium silicate phase with molar ratio 5 had a hardness of 194HV10, which was the highest one. As the molar ratio decreased the hardness also decreased reaching the value of 82HV10 at a molar ratio 4.1 which corresponded to a sodium silicate gel with substantial solubility ($\approx$45% silicon dissolution). Macroscopic hardness is generally interrelated to intermolecular bonds and comprises a measure of the resistance offered by the materials to being indented. The resistance to indentation in the case of brittle materials like the sodium silicate gels was attributed to the energy expended in crack formation and propagation [33]. Stronger intermolecular bonds between

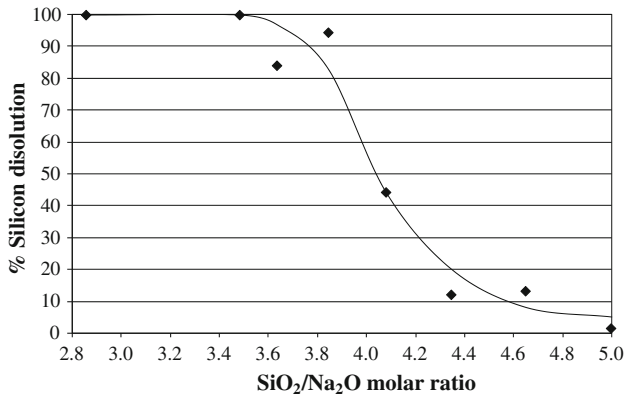

Fig. 8 Solubility of sodium silicate gels as a function of the SiO_2/Na_2O molar ratio (24 h, ambient temperature, deionized water)

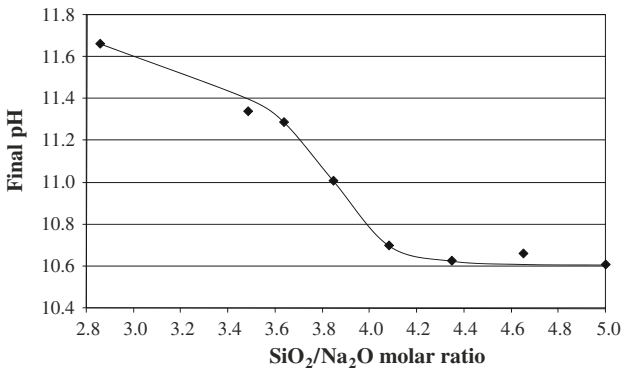

Fig. 9 pH of solutions after the end of dissolution tests as a function of the SiO_2/Na_2O molar ratio

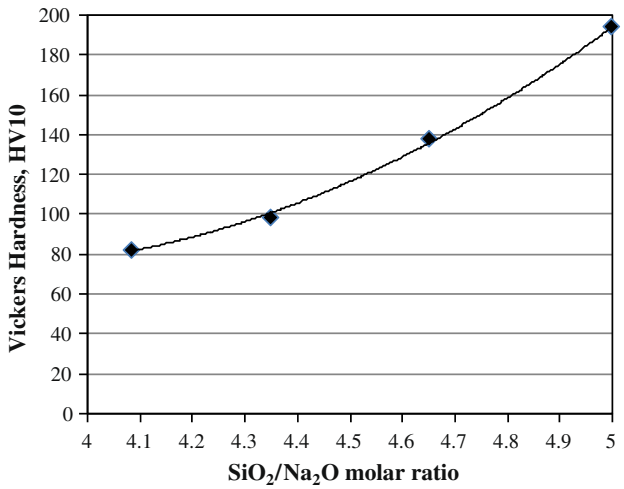

Fig. 10 Vickers hardness of sodium silicate gels as a function of the SiO_2/Na_2O molar ratio

the structural units of sodium silicate gel necessitated higher energy consumption for crack formation and propagation and had as a result higher hardness values. Therefore, the structure of sodium silicate gels was strongly interrelated to their hardness. The sodium silicate gel (SiO_2/Na_2O molar ratio 5) with structural units centered on SiQ^3 units had its silicon atoms strong bonded and thus exhibited the highest hardness. As the SiO_2/Na_2O molar ratio decreased, there was a shift of the structural units toward SiQ^2 units which had the silicon atoms less strong bonded and therefore exhibited lower hardness. Additionally, Vickers hardness can be used as a measure of the compressive strength of the sodium silicate gels. Although there is a lack of an accurate mathematical correlation between Vickers hardness and compressive strength, it is generally accepted that Vickers hardness and compressive strength are qualitatively analogue quantities [34–36]. Therefore, it was concluded that the SiO_2/Na_2O molar ratio governs the structure of the sodium silicate gels and consequently affects their mechanical properties. The higher the SiO_2/Na_2O molar ratio in the sodium silicate gels, the higher their Vickers hardness and compressive strength are.

Al effect on structure and properties of gelatinous phase

The effect of aluminum addition on the hydrolytic stability of prepared gels is shown in Fig. 11. The sodium aluminosilicate gels were prepared by mixing sodium silicate with aluminum chloride solutions. It was clearly observed that the solubility of all aluminosilicate gels were substantially lower than the corresponding ones of the silicate gels. Additionally, as the Si/Al molar ratio decreased the solubility was substantially decreased. Unfortunately, from this kind of experiments it was not feasible to attribute definitely the improved gel's hydrolytic stability to aluminum incorporation. As seen in Fig. 12, all prepared gels contained crystalline sodium and aluminum chloride phases, indicating that the whole amount of added aluminum was not incorporated in the aluminosilicate gels. Additionally, the aluminum incorporation in gels was accompanied by the formation of sodium chloride salt, indicating the removal of sodium from the gels and thus the increase in the SiO_2/Na_2O molar ratio in them. The above observations were strengthened by the results of the infrared analysis shown in Fig. 13. The three absorption bands of Fig. 4, which comprise the fingerprint of silicate gel, were also observed in Fig. 13. The strong shift of the peak of band I from 1027 cm^{-1} for a sodium silicate gel with molar ratio $SiO_2/Na_2O = 4.08$ to 1090 cm^{-1} as the Si/Al molar ratio in the sodium aluminosilicate gel decreased could be attributed principally to the increased SiO_2/Na_2O molar ratio in the prepared gels due to sodium removal and secondarily to the existence of NaCl which has two absorption peaks in the region 1025–1102 cm^{-1}. This conclusion was strengthened by the shift of bands II and III that are unique for silicate gels, toward higher wavenumbers which was consistent with the trend shown in Fig. 4. As a conclusion, the prepared aluminosilicate gels at different Si/Al molar ratios had substantially higher SiO_2/Na_2O molar ratios than

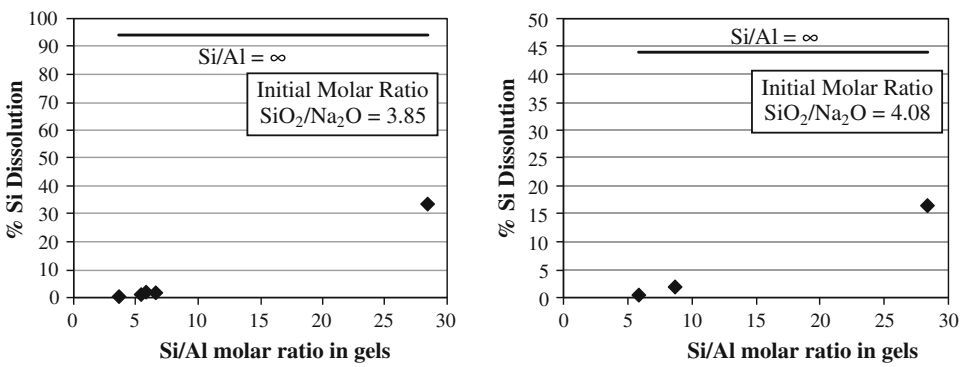

Fig. 11 Silicon dissolution as a function of Si/Al molar ratio of gels (24 h, ambient temperature, deionized water)

the initial one of 4.08 and therefore their hydrolytic stability was significantly improved according to the trend shown in Fig. 8.

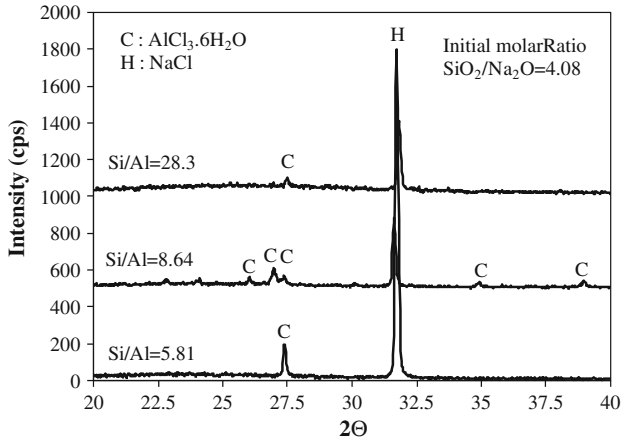

Fig. 12 XRD patterns of aluminosilicate gels as a function of Si/Al molar ratio (initial molar ratio $SiO_2/Na_2O = 4.08$)

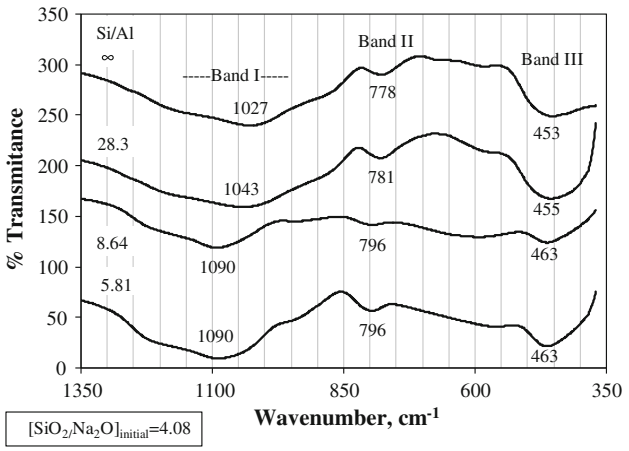

Fig. 13 FTIR spectra of produced gels as a function of the Si/Al molar ratio in the range 370–2000 cm^{-1} (initial molar ratio $SiO_2/Na_2O = 4.08$)

In order to elucidate the role of added aluminum on the structure and properties of sodium aluminosilicate gels, three new gels were prepared by mixing sodium silicate with sodium aluminate solutions. Under that condition the sodium removal from the gels was avoided and therefore all aluminosilicate gels had the same SiO_2/Na_2O molar ratio. The sodium aluminosilicate gels with molar ratio $SiO_2/Na_2O = 7.5$ and Si/Al molar ratios ranging from 5.7 to 53.2 were characterized as X-ray amorphous materials as seen in Fig. 14a. There was a lack of sharp diffraction peaks and the X-ray diffractograms were consisted of a broad diffuse halo peak which was registered between $2\theta = 14$ and 35°. The halo peak had its maximum around $2\theta = 23°$ independently of the Si/Al molar ratio indicating that the sodium aluminosilicate gels with molar ratio $SiO_2/Na_2O = 7.5$ were composed primarily from SiQ^4 and SiQ^3 structural units following the general trend shown in Fig. 2. The FTIR spectra shown in Fig. 14b elucidated more the structure of prepared sodium aluminosilicate gels. The band I was very broad reflecting the amorphous character and thus the wide distribution of SiQ^n structural units in the prepared sodium aluminosilicate gels. The FTIR spectra showed a maximum absorption in the range 1080–1094 cm^{-1} which was located closer to the absorption bands of SiQ^4 and SiQ^3 structural units, indicating their predominance in the prepared sodium aluminosilicate gels. The effect of Si/Al molar ratio on the absorption band I was noteworthy. As the Si/Al molar ratio decreased from 53.2 to 5.7, the band I became broader and gradually shifted toward higher wavenumbers, indicating an aluminosilicate structure richer in SiQ^4 structural units probably due to higher crosslinking offered by the presence of aluminum [37]. The absorption bands II and III were centered at higher wavenumbers in relation to the ones of silicate gels with lower SiO_2/Na_2O molar ratios following the general trend shown in Fig. 4 and seemed to be insusceptible of the Si/Al molar ratio. The hydrolytic stability of sodium aluminosilicate gels as a function of the Si/Al molar ratio is shown in Fig. 15. Although the water solubility of silicate

Fig. 14 **a** XRD patterns and **b** FTIR spectra of sodium aluminosilicate gels with molar ratio $SiO_2/Na_2O = 7.5$ as a function of Si/Al molar ratios

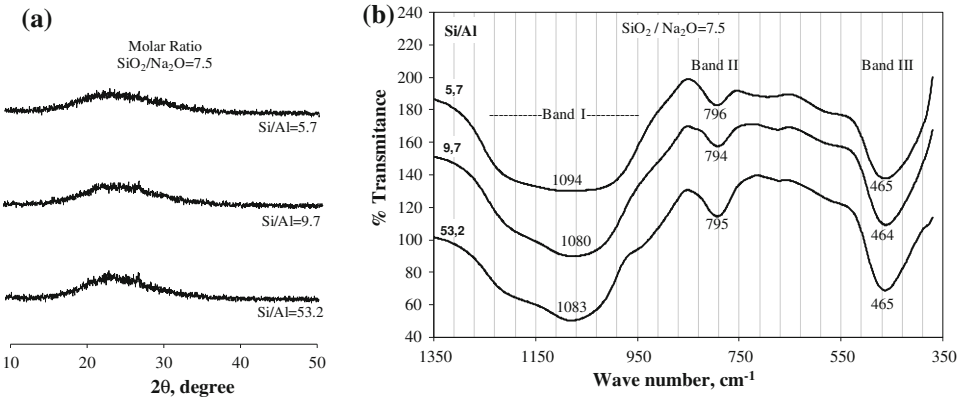

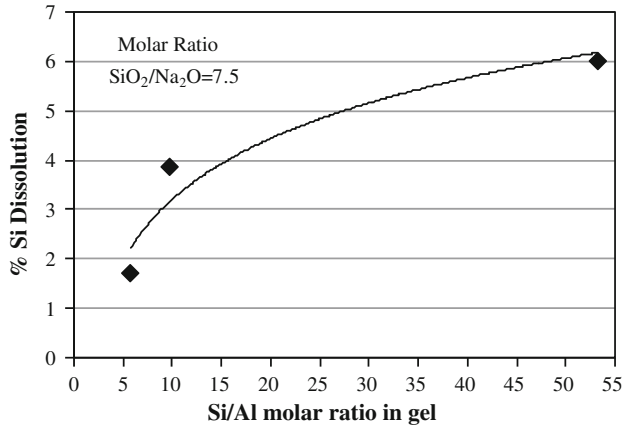

Fig. 15 Silicon dissolution as a function of Si/Al molar ratio of aluminosilicate gels with molar ratio $SiO_2/Na_2O = 7.5$ (24 h, ambient temperature, deionized water)

gels with high SiO_2/Na_2O molar ratios is limited, the results showed a substantial decrease in their solubility with the incorporation of aluminum. This observation was in accordance with an aluminosilicate gel richer in SiQ^4 structural units and highly crosslinked [38] as it was concluded by the FTIR analysis.

Geopolymerization process

The geopolymerization process involves a heterogeneous chemical reaction between two phases; (a) a fine solid aluminosilicate phase and (b) an aqueous alkali silicate solution. Geopolymers are normally composite materials consisting of two discrete phases: (a) non-dissolved solid grains and (b) a gelatinous binder. The non-dissolved solids are attributed either to insoluble solid phases existing in the initial solid aluminosilicate raw material or to incomplete dissolution due to slow reaction kinetics. The gelatinous phase binding the non-dissolved solid grains is principally of aluminosilicate nature although other metals such as Ca, Fe, etc., could be found as minor constituents in the gel. A good geopolymer has to have at least two properties: (a) high hydrolytic stability and (b) satisfactory mechanical strength (compressive, flexural, etc.) depending on the type of application. Both properties depend on the structure of the gelatinous binder. This study proved that the hydrolytic stability and the compressive strength of silicate gels are strongly correlated to the SiO_2/Na_2O and Si/Al molar ratios. Water stable silicate gels with Si dissolution <10% can be produced at SiO_2/Na_2O molar ratios >4.6. The incorporation of aluminum in the gel structure can substantially increase the hydrolytic stability probably even for low SiO_2/Na_2O molar ratios [38]. Taking into account that the commercially available sodium silicate solutions has a SiO_2/Na_2O molar ratio in-between 2 to 3.5, it can be concluded that in order to produce a water resistant and high strength geopolymer either the initial aqueous alkali silicate phase must be doped in silicon and aluminum or the raw solid aluminosilicate phase must contain big amount of easily dissolved silicon and aluminum. The first alternative is an expensive one and is advisable for the synthesis of high added value materials (e.g., fire resistant materials) utilizing a solid non-reactive siliceous phase as a filler. The doping of initial aqueous alkali silicate phase must be performed by the addition of either silica fumes, which is a highly reactive glassy material and/or sodium aluminate solution. The second alternative is the one often used in the synthesis of geopolymeric materials. There is a big variety of raw solid aluminosilicate materials (industrial minerals or industrial solid residues and wastes) that contain big amount of amorphous reactive phases which are easily soluble in the initial aqueous alkali silicate phase liberating several aluminosilicate species and creating through evaporated polycondensation a binder with the desirable SiO_2/Na_2O and Si/Al molar ratios. In such systems the doping of the initial aqueous alkali silicate phase with NaOH is essential in order to achieve high alkalinity and thus high initial Si and Al dissolution rates. In case of a raw solid aluminosilicate material with intermediate reactivity in alkaline solutions, a portion of it is normally replaced by a highly reactive material, such as metakolin, in order to improve the dissolution process and thus produce a gelatinous binder with the desirable SiO_2/Na_2O and Si/Al molar ratios.

A simplified flow diagram for the synthesis of geopolymers normally includes (a) mechanical pretreatment of raw solid aluminosilicate material (crushing and grinding), (b) preparation of initial aqueous alkali silicate phase, (c) mixing of solid and aqueous phases, (d) molding of pastes, (e) curing at low to moderate temperatures (40–80 °C) for several hours, and (f) setting at environment. The production cost of geopolymers is dependent more on the cost of used chemicals and less on the cost of consumed energy and labor. The cost of used chemicals is in-between 60 to 80% of the total production cost depended on the type of the geopolymeric system. Almost 80–90% of the cost of chemicals is attributed to the cost of the used sodium silicate solution. Taking into account the above estimates which have been drawn for a ferronickel slag- and a red mud/metakaolin-based geopolymeric systems [8, 9], it can be concluded that the economic production of geopolymers must follow the direction of the substantial decrease in the amount of utilized sodium silicate solution. This target could be achieved by decreasing substantially the minimum SiO_2/Na_2O molar ratio above which the binding gels exhibit substantial hydrolytic stability. Toward this direction, the study of the effect of several additives such as elements from group 13 (B, Al) and group 15 (P) of the periodic table as well as transition metals such as Fe, Cr,

Ni, etc., on the gelatinous binder structure and properties could be very useful.

Conclusions

The structure of silicate gels produced by accelerated polycondensation in sodium silicate solutions is dependent on SiO_2/Na_2O molar ratio. Sodium ions are network modifying agents affecting the number of NBO atoms in the first coordination sphere of silicon atoms and thus the relative distribution of SiQ^n ($n = 0$–4) structural units in the sodium silicate gels. In general, low SiO_2/Na_2O molar ratios favor the predominance of SiQ^2, SiQ^1 structural units over the other SiQ^n ones, whereas high SiO_2/Na_2O molar ratios create a SiQ^n structural units distribution around SiQ^3, SiQ^4 ones. Preliminary experiments showed that aluminum incorporation in sodium aluminosilicate gels affects their structure. Aluminosilicate gels are richer in SiQ^4 structural units and more crosslinked as the Si/Al molar ratio decreases.

The water that remains in the sodium silicate gels after accelerated polycondensation is associated mainly with physically bound water on silanol groups and secondary with surface hydroxyl groups from the internal and vicinal hydrogen-bonded silanol groups. The first type of incorporated water in gels is totally removed up to 150 °C, whereas the latter ones are completely removed at temperatures as high as 500 °C. Therefore, the sodium silicate and aluminosilicate gels are highly endothermic materials because they can absorb large amounts of heat and use it as latent energy for the vaporization of water.

The structure of sodium silicate gel is strongly correlated to its properties. The hydrolytic stability of sodium silicate gels is dependent on SiO_2/Na_2O molar ratio. The higher the molar ratio, the higher the hydrolytic stability is. Sodium silicate gels with molar ratio >4.4 are characterized as practically insoluble in water and therefore exhibit very high hydrolytic stability. Preliminary experiments showed that the hydrolytic stability of gels is substantially improved by the incorporation of aluminum. The lower the Si/Al molar ratio, the higher the hydrolytic stability is. Finally, the Vickers hardness of gels, a quantity that can be used as an indirect measure of compressive strength of gels, proved to be SiO_2/Na_2O molar ratio dependent. The higher the SiO_2/Na_2O molar ratio in the sodium silicate gels, the higher their Vickers hardness and compressive strength are.

Based on the above findings it was concluded that in order to produce a water resistant and high strength geopolymer the initial strong alkaline aqueous phase must be enriched in soluble SiO_2 by mixing with sodium silicate solution. Based on previous geopolymerization studies, it was estimated that the most important production cost factor is the cost of used chemicals and especially the one of sodium silicate solution. Consequently, economic production of geopolymers means substantially decrease in the amount of used sodium silicate solution for their production. This target could be achieved by decreasing substantially the minimum SiO_2/Na_2O molar ratio above which the binding gels exhibit substantial hydrolytic stability. Therefore, it could be very useful for the geopolymerization technology the understanding of the effect of several additives such as elements from group 13 (B, Al) and group 15 (P) of periodic table as well as transition metals such as Fe, Cr, Ni, etc., on the gelatinous binder structure and its properties.

Acknowledgement The authors would like to thank the Senator Committee of Basic Research of the National Technical University of Athens, Programme "PEBE-2007", R.C.·No.:65/1634 for the financial support of this study.

References

1. Davidovits J (1999) Geopolymer '99 2nd international conference, Saint-Quentin, France, pp 9–39
2. Xu H (2002) PhD Thesis, Department of Chemical Engineering, University of Melbourne
3. Davidovits J (2005) Proceedings of the world congress geopolymer 2005, Saint-Quentin, France, pp 9–15
4. Palomo A, Grutzeck MW, Blanco MT (1999) Cem Concr Res 29:1323
5. Cheng TW, Chiu JP (2003) Miner Eng 16:205
6. Pacheco-Torgal F, Castro-Gomes JP, Jalali S (2005) Proceedings of the world congress geopolymer 2005, Saint-Quentin, France, pp 93–98
7. Panias D, Giannopoulou IP, Perraki T (2007) Colloids Surf A Physicochem Eng Aspects 301:246
8. Maragkos I, Giannopoulou IP, Panias D (2009) Miner Eng 22:196
9. Dimas D, Giannopoulou IP, Panias D (2009) Miner Process Extr Metall Rev (in press)
10. Davidovits J (2008) Geopolymer chemistry & applications, 2nd edn, chapters 15–16. Institute Géopolymère, Saint-Quentin, pp 333–365
11. McCormick AV, Bell AT, Radke CJ (1989) J Phys Chem 93(5): 1737
12. Duxson P, Fernandez-Jimenez A, Provis JL, Luckey GC, Palomo A, van Deventer JSJ (2007) J Mater Sci 42:2917. doi:10.1007/s10853-006-0637-z
13. Aagard P, Helgeson HC (1982) Am J Sci 282:237
14. Phair JW, Van Deventer JSJ (2002) Int J Miner Process 66:121
15. Davidovits J (2008) Geopolymer chemistry & applications, 2nd edn, chapter 4. Institute Géopolymère, Saint-Quentin, pp 61–65
16. Davidovits J (1999) Proceedings of the geopolymer international conference 1999, Saint-Quentin, France, pp 9–40
17. Warren BE, Biscoe L (1938) J Am Ceram Soc 21(2):49
18. Warren BE, Loring AD (1935) J Am Ceram Soc 18(1–12):269
19. Baes CF, Mesmer RE (1976) The hydrolysis of cations. Wiley, New York, pp 336–342
20. Sefcik J, McCormick AV (1997) Ceram Process 43:2773
21. Knight CTG, Balec RJ, Kinrade SD (2007) Angew Chem 119:8296
22. Bass JL, Turner GL (1997) J Phys Chem B 101:10638

23. Florke OW et al (2008) Silica, Ullmann's encyclopedia of industrial chemistry. Wiley-VCH Verlag GmbH & Co., Weinheim
24. Elliott SR (2001) Amorphous materials: medium-range order, encyclopedia of materials: science and technology. Elsevier Science Ltd., pp 215–220
25. Hadke M, Mozgawa W (1993) Vib Spectrosc 5:75
26. Clayden NJ, Esposito S, Aronne A, Pernice P (1999) J Non-Cryst Solids 258:11
27. Lecomte I, Henrist C, Liegeois M, Maseri F, Rulmont A, Cloots R (2006) J Eur Ceram Soc 26:3789
28. Sitarz M, Handke M, Mozgawa W (2000) Spectrochemica Acta A 56:1819
29. Iler RK (1979) The chemistry of silica. Wiley, New York
30. Morrow BA, McFarlan AJ (1991) Langmuir 7:1695
31. Burneau A, Barres O, Gallas JP, Lavalley JC (1990) Langmuir 6: 1364
32. Jantzen CM, Plodinec MJ (1984) J Non-Cryst Solids 67:207
33. Sundararajan G, Roy M (2001) Hardness testing, encyclopedia of materials: science and technology. Elsevier Science Ltd., Amsterdam, pp 3728–3736
34. Richerson DW (1992) Modern ceramic engineering: properties, processing and use in design. Marcel Dekker, pp 179
35. Yamasaki TK, Nishioka M, Yanagisawa K, Ioku K (1992) J Mater Sci Lett 11(4):233
36. Park CY, Yoon SD, Yun YH (2007) J Ceram Process Res 8(6):435
37. Ischenko V, Harshe R, Riedel R, Woltersdorf J (2006) J Organomet Chem 691:4086
38. Davidovits J (2008) Geopolymer chemistry & applications, 2nd edn, chapter 26. Institute Géopolymère, Saint-Quentin, pp 547–574